REPORT NO. P77-490
HAC Ref. NO. D9802

ELECTRO-OPTICAL AND DATA SYSTEMS GROUP
HUGHES
HUGHES AIRCRAFT COMPANY

# 4.3 MICROMETER LASER DEMONSTRATION EXPERIMENT

HUGHES AIRCRAFT COMPANY
CULVER CITY, CALIFORNIA 90230

OCTOBER 1977

Interim Technical Report for Period
29 June 1977 – 30 September 1977





SPONSORED BY
Defense Advanced Research Projects Agency
ARPA Order No. 2062, Amendment No. 16

MONITORED BY
Mr. Wayne Whitney, NRL Code 5540, under
Contract No. N00173-77-C-0174





CONTRACT EFFECTIVE DATE: 29 June 1977
CONTRACT EXPIRATION DATE: 31 Jenuery 1978

# REPORT DOCUMENTATION PAGE

READ INSTRUCTIONS BEFORE COMPLETING FORM

| | |
|---|---|
| 1. REPORT NUMBER: HAC-P77-490, HAC-REF-D9802 | 2. GOVT ACCESSION NO. |
| 3. RECIPIENT'S CATALOG NUMBER | |
| 4. TITLE (and Subtitle): 4.3 MICROMETER LASER DEMONSTRATION EXPERIMENT, | 5. TYPE OF REPORT & PERIOD COVERED: Interim Report [illegible] Jun[illegible] - 30 Sep[illegible] 77, |
| | 6. PERFORMING ORG. REPORT NUMBER: P77-490 |
| 7. AUTHOR(s): Philip K. Baily, Jack Finzi | 8. CONTRACT OR GRANT NUMBER(s): N00173-77-C-0174, [illegible] |
| 9. PERFORMING ORGANIZATION NAME AND ADDRESS: Hughes Aircraft Company, Centinela and Teale Sts., Culver City, CA 90230 | 10. PROGRAM ELEMENT, PROJECT, TASK AREA & WORK UNIT NUMBERS: ARPA Order [illegible]-2062, AMENDMENT No. 16 |
| 11. CONTROLLING OFFICE NAME AND ADDRESS: Advanced Research Projects Agency, 1400 Wilson Blvd., Arlington, Virginia | 12. REPORT DATE: Oct[illegible] 77 |
| | 13. NUMBER OF PAGES: 25 (12) 37 p. |
| 14. MONITORING AGENCY NAME & ADDRESS (if different from Controlling Office): Naval Research Laboratory, 4555 Overlook Ave. S.W., Washington, D.C. | 15. SECURITY CLASS. (of this report): Unclassified |
| | 15a. DECLASSIFICATION/DOWNGRADING SCHEDULE |

16. DISTRIBUTION STATEMENT (of this Report)

[redacted]

[illegible] STATEMENT A
Approved for public release;
Distribution Unlimited

17. DISTRIBUTION STATEMENT (of the abstract entered in Block 20, if different from Report)

None

18. SUPPLEMENTARY NOTES

None

[illegible] JAN 6 1978

19. KEY WORDS (Continue on reverse side if necessary and identify by block number)

Carbon Dioxide Laser
Chemical Laser
Optical Pumping
Collisional Energy Transfer

20. ABSTRACT (Continue on reverse side if necessary and identify by block number)

The possibility of converting multiline CW DF chemical laser radiation to single line CW 4.3 micrometer radiation by means of an Optical Resonance Pumped Transfer Laser (ORTL) is investigated. The ORTL medium consists of a DF and $CO_2$ mixture and a suitable diluent. The optically pumped DF collisionally transfers its vibrational excitation to the $CO_2$. This program is concerned with a demonstration of 4.3μm oscillation between the (0001) and ground state $CO_2$ levels. During this reporting period, a laser demonstration experiment has been designed and hardware is being

DD FORM 1 JAN 73 1473 EDITION OF 1 NOV 65 IS OBSOLETE

[illegible]

SECURITY CLASSIFICATION OF THIS PAGE (When Date Entered)

409084

20. ABSTRACT (continued)

assembled. DF and $CO_2^{\prime\prime}$ fluorescence experiments were performed as a guide to the experimental design. The experiments and results are discussed. The results indicate a strong probability of success for the demonstration experiment.

Letter on file

A

## SUMMARY

High energy chemical lasers are prime candidates for space laser systems and for other applications, because they are very efficient generators of high power laser radiation. The multiline output characteristic of these lasers is, however, detrimental to modern active phase control techniques that may be essential for achieving the ultimately required beam focusing. Optical Resonance pumped Transfer Lasers (ORTL) may offer a simple and practical solution to this problem by efficiently converting the multiline DF chemical laser power into a single line output. Specifically, theoretical analysis indicates that power conversion efficiency of 70 percent may be achieved in converting 3.8 μm average wavelength DF chemical laser power into single line output near 4.3 μm in a DF/$CO_2$ ORTL. The 4.3 μm laser output originates from the $CO_2$ $(00^0 1) \rightarrow (000)$, transition and therefore requires inversion relative to the $CO_2$ ground state. The goal of this program is to demonstrate laser action in this transition in order to show principle feasibility.

During this first program period an ORTL apparatus suitable for demonstrating $CO_2$ 4.3 μm lasing has been assembled and first test results have been achieved. In a series of experiments we have attempted to verify that measured population ratios of the $CO_2$ levels, $(00^0 1)/(00^0 0)$ can in fact attain or exceed the value of one, which is necessary to achieve lasing in this band. In a second experiment we will attempt to lase the 4.3 μm transition. Analysis of fluorescent data at 10.6 μm and 4.3 μm radiation obtained from a 3 mm ORTL cell pumped by a 200 watt chemical DF laser indicates that ratios of greater than unity were most likely achieved in these experiments. The uncertainty of the data reduction is due to complications arising from the as yet unknown levels of excitation of higher order $CO_2$ states that also could contribute to 10.6 μm fluorescent emissions. Preparations on the second experiment have progressed and a first attempt at demonstrating laser action at 4.3 μm will be made in October.

# PREFACE

The work discussed in this report is based upon proprietary prior work supported by Hughes Internal Research and Development funds. In addition, work supported by the Ballistic Missile Defense Advanced Technology Center under Contract DASG60-77-C-0056 has strongly influenced the technical approach on the present program. This report was authored by P.K. Baily and J. Finzi. The authors would like to acknowledge the technical guidance provided by F.N. Mastrup, and numerous technical discussions with G. Holleman and J. Wang. We would also like to acknowledge the assistance of K. Hui, H. Injeyan, C. Lovejoy, R. Shimazu, and L. Williams in performing the fluorescence experiments.

CONTENTS

## LIST OF ILLUSTRATIONS



## LIST OF TABLES

# 1.0 INTRODUCTION

High energy chemical lasers in advanced space systems are presently under active consideration by ARPA and other government agencies. In such systems the beam degrading effects resulting from propagation through the atmosphere do not exist at all or are greatly reduced. Therefore, the ability of the laser system to deliver near ultimate irradiance levels to distant targets at prescribed output power levels depends only on the extracted beam quality, the output optics size and, last but not least, on the attainable precision in pointing and tracking. Modern chemical space laser concepts involve cavity resonators, such as the cylindrical configuration, where satisfactory "mode" control or, more precisely, the ability of the resonator to outcouple a near diffraction limited beam is questionable or uncertain. Achievement of the required precision in pointing and tracking may require single line operation once adaptive optics approaches are seriously pursued for beam focusing. This is so because the active phase control of a selected line from amongst the large number of emitted high energy chemical laser lines does not at all imply control of the entire multiline beam. It is much more likely that successful active phase control of a chemical laser powered device beam will only be possible when the output is in fact single line.

The related problems of beam control and single line operation are both amenable to solution by the Optical Resonance Pumped Transfer Laser (ORTL) concept. The ORTL concept (Figure 1) promises to permit one to convert from high efficiency multiline, low optical quality, "multimode" CW primary laser cavity power to single line, CW low divergence laser output power. This is accomplished by arranging for the primary, multiline DF (HF) power to oscillate between two highly reflective mirrors as shown in Figure 1. The ORTL cell, which is placed within this trapped DF (HF) laser radiation field becomes, in a well designed ORTL, the major primary power sink. Effective resonance absorption in the ORTL cell is achieved by mixing a well balanced amount of DF (HF) gas into the ORTL gas. The multiline, primary DF (HF) laser power absorbed by the DF (HF) donors is subsequently transferred by V-V collisions to an acceptor molecule which becomes the lasing molecule for the single line output (ORTL)

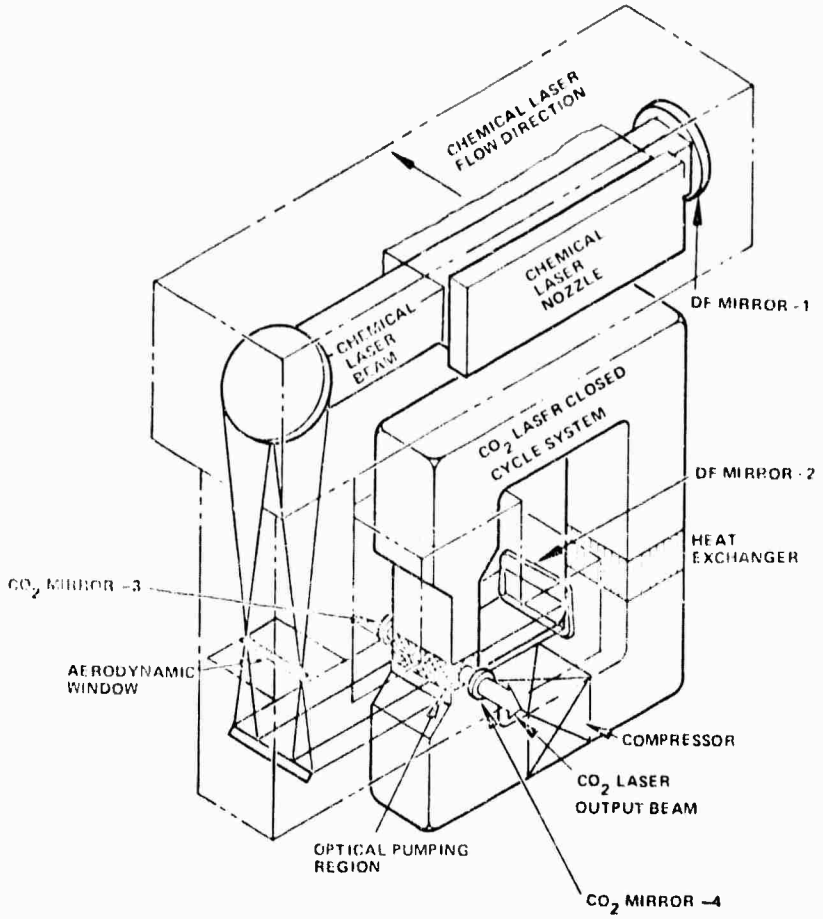


Figure 1. Optical Resonance Pumped Transfer Laser (ORTL) concept.

laser. Expectations of better beam quality are a consequence of the resonant absorption of optical radiation; this minimizes the heating of the ORTL medium and good medium homogeneity can be maintained. This is especially true if the primary and ORTL radiation are very close in wavelength. Additional advantages of the ORTL technique arise from the fact that unusual excitation conditions can be generated capable of simultaneously producing both single line output and efficient power transfer. In addition, very high volumetric (Megawatt/liter active volume) power output levels appear to be realizable. The closed cycle ORTL concept would allow the use of unusual gases as ORTL laser sources. These might include isotopically

enriched substances or substances which should not be discharged into the atmosphere at high rates because of their explosive or toxic nature.

The intracavity ORTL concept was first demonstrated at Hughes in June, 1976* with a DF laser as the primary source of radiation and $CO_2$ as the ORTL medium. Oscillation was achieved at 10.6 microns. The significant advances associated with this demonstration were three:

- the ORTL was pumped continuously by DF primary laser power, obtaining CW 10.6μm lasing as opposed to pulsed $CO_2$ operation in previous work
- multiline, CW optical pumping was used specifically for enforcing a primary pump radiation field controlled donor (DF) vibrational level distribution in the transfer laser medium such that effective multiline pumping with DF laser power could occur
- the necessary high pump radiation flux (Watt/$cm^2$) was achieved by locating the DF/$CO_2$ transfer laser medium inside the closed cavity DF laser resonator mirrors, thus demonstrating the important intracavity configuration and concept.

This 10.6 μm or DF/$CO_2$ ORTL is not very practical for applications specifically requiring efficient space lasers, however, because of the inherent and unavoidable power loss associated with converting DF power at an average wavelength of 3.8 μm to 10.6 μm $CO_2$ laser radiation. This power loss occurs because all energy transfer processes in the ORTL medium are quantum effects and, therefore, the maximum possible ORTL output power to ORTL input power ratio is limited by the wavelength ratio. Another ORTL with a more favorable, i.e., shorter, output wavelength was therefore needed. In the special case of DF/$CO_2$ ORTL's very reliable predictions on the transfer of DF excitation to the $CO_2$ ($00^0 1$) level could be made because of the detailed and quantitative knowledge of the involved kinetics. Such analysis indicated that mixing ratios and pressures could be defined where over 90 percent of the optically pumped DF level energy would be transferred to the $CO_2$ ($00^0 1$) level. Shorter wavelength lasing could be accomplished if it

---

*J. H. S. Wang, J. Finzi, and F. N. Mastrup, Appl. Phys. Lett. 31, 35 (1977)

were possible to enforce effective lasing from $CO_2$ ($00^0 1$) to a level close to the ground state or to the ground state itself. Further theoretical work at Hughes clearly indicated the possibility of effective lasing in the $CO_2$ 4.3 μm band with a multiline DF-to-single line 4.3 μm power conversion efficiency as high as 70 percent. The only uncertainty was the uncertain role of V-V collisions in the $CO_2$ ORTL component.

The high efficiencies potentially achievable in this "two-level" system lead to a preliminary investigation of the scalability of such a laser system. Largely under the sponsorship of Hughes IR&D, a model, confirmed by experiment, has been developed that describes adequately the complicated interaction of the multiline pump (DF) laser and the ORTL both situated in the same DF-trapped radiation field. The main features of the model are:

- It describes the interaction of the pump (HF) laser and the ORTL in closed cavity;
- It defines stability criteria for this interaction;
- It permits the detailed prediction of ORTL output power and multiline pump power-to-single-line ORTL output power conversion efficiency;
- It couples the combined optical pump (trapped) and ORTL (output laser) radiation field to relevant ORTL cavity optical design and flow field parameters.

The relevant DF and $CO_2$ vibrational energy level structure and the model performance prediction for a "two-level" 4.3 micron $CO_2$ ORTL are shown in Figures 2, 3, and 4. As can be seen from Figure 3, for favorable conditions power conversion efficiencies from 3.8 μm average wavelength, multiline DF chemical laser pump power into single line ORTL output power at 4.3 μm of over 70 percent are predicted. Calculated output power referred to unit volume, as read from Figure 4, is close to 1.7 megawatt/liter at room temperature with an optical pump flux of 90 kw/cm$^2$ at the ORTL cell. The potential impact of this technology on high energy lasers may be further appreciated when sizing a sample high energy ORTL: Assume the DF-laser to deliver 230 kw, multimode closed cavity power (Figure 1); assume the ORTL cell (Figure 1) to have dimensions of 10 cm x 3.16 cm x 3.16 cm

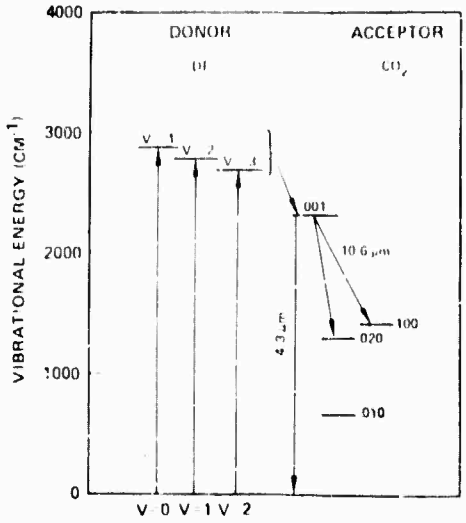


Figure 2. $DF/CO_2$ energy transfer level diagram.

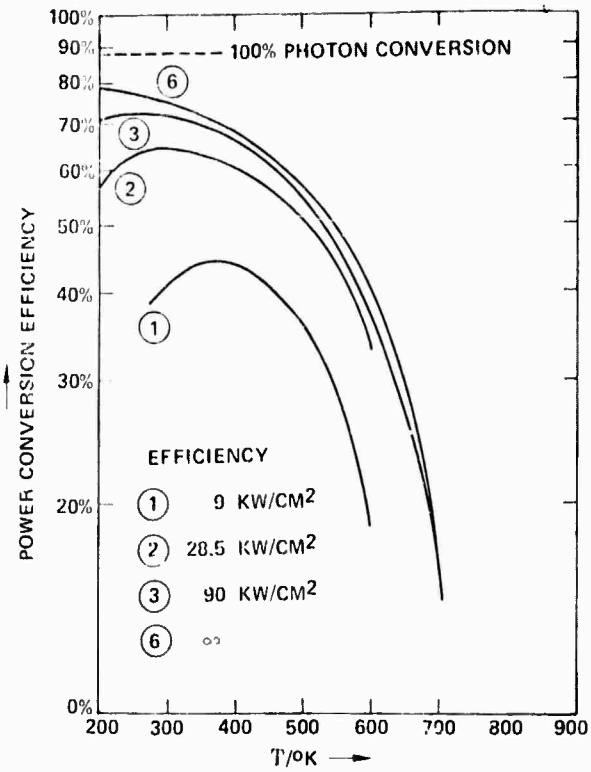


Figure 3. Predicted power conversion efficiencies (pressure = 1/3 Atm, $H_2$:$CO_2$DF = 93:6:1 mole concentration; normalized outcoupling = 4.25%/cm.)

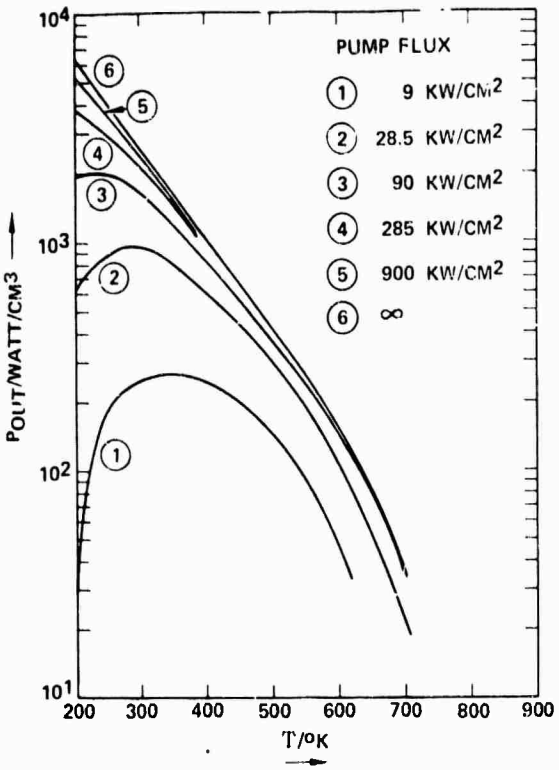


Figure 4. Predicted output power per unit volume (conditions are the same as in Figure 3).

(0.1 liter); assume the ORTL gas to be at 1/3 atm pressure and let the gas mixture consist of 1 percent DF, 6 percent $CO_2$ and 93 percent $H_2$ diluent; assume the ORTL gas injection velocity to be $4 \times 10^4$ cm/sec and inlet temperature 300°K ($M^2 = 0.1$); assume the ORTL cavity to exhibit 85 percent outcoupling. The expected ORTL output is, for the cited conditions, 160 kw, at 4.3 μm; the calculated conversion efficiency is 70 percent. The temperature rise of the ORTL gas flowing through the excitation region is only 130°K, raising the ORTL exit temperature to 430°K. Of particular interest is the small size of the ORTL (0.1 liter), the low flow velocity, the comparatively modest medium temperature rise and, of course, the single line output. All these features combine to make the ORTL concept exceptionally convenient for application of advanced mode control techniques.

## 2.0 PROGRAM OBJECTIVES

The major objectives of the 4.3 Micrometer Laser Demonstration Experiment Program are to:

- Demonstrate and characterize 4.3 μm $CO_2$ lasing action in a DF laser pumped DF/$CO_2$ ORTL.
- Assess, through comparison with theoretical analysis, the gross effects of V-V collisions in this system.
- Define the need for future and refined work, if any, in this technology area as applied to the chemical space laser ORTL.

The major technical problem is associated with the uncertain effects of $CO_2$ – $CO_2$ V-V collisions. To successfully achieve the objectives the program was defined in terms of four work tasks as follows:

1. Apparatus Modification and Experimental Design
2. 4.3 Micrometer CW DF/$CO_2$ ORTL Demonstration
3. 4.3 Micrometer CW DF/$CO_2$ ORTL Characterization
4. Data Analysis and Evaluation

During this reporting period major results have been achieved as part of Tasks 1 and 2.

## 3.0 FLUORESCENCE EXPERIMENTS

As an aid in the design of the laser demonstration experiment, fluorescence experiments were performed. These experiments consisted of the observation of 4.3 μm and 10.6 μm fluorescence from an ORTL cell (without resonator optics) irradiated by DF laser radiation. Data was taken under a number of conditions and then analyzed to ascertain the excited state $CO_2$ population densities in order to choose the optimal lasing conditions. These experiments will be discussed below.

### 3.1 APPARATUS DESCRIPTIONS

A photograph of the apparatus and a schematic diagram of the fluorescence experiment are shown in Figure 5 and Figure 6. A flowing $DF/CO_2/He$ mixture was introduced into the ORTL cell through a 0.30 cm circular duct. For these experiments, the ORTL cell was external to the DF pump

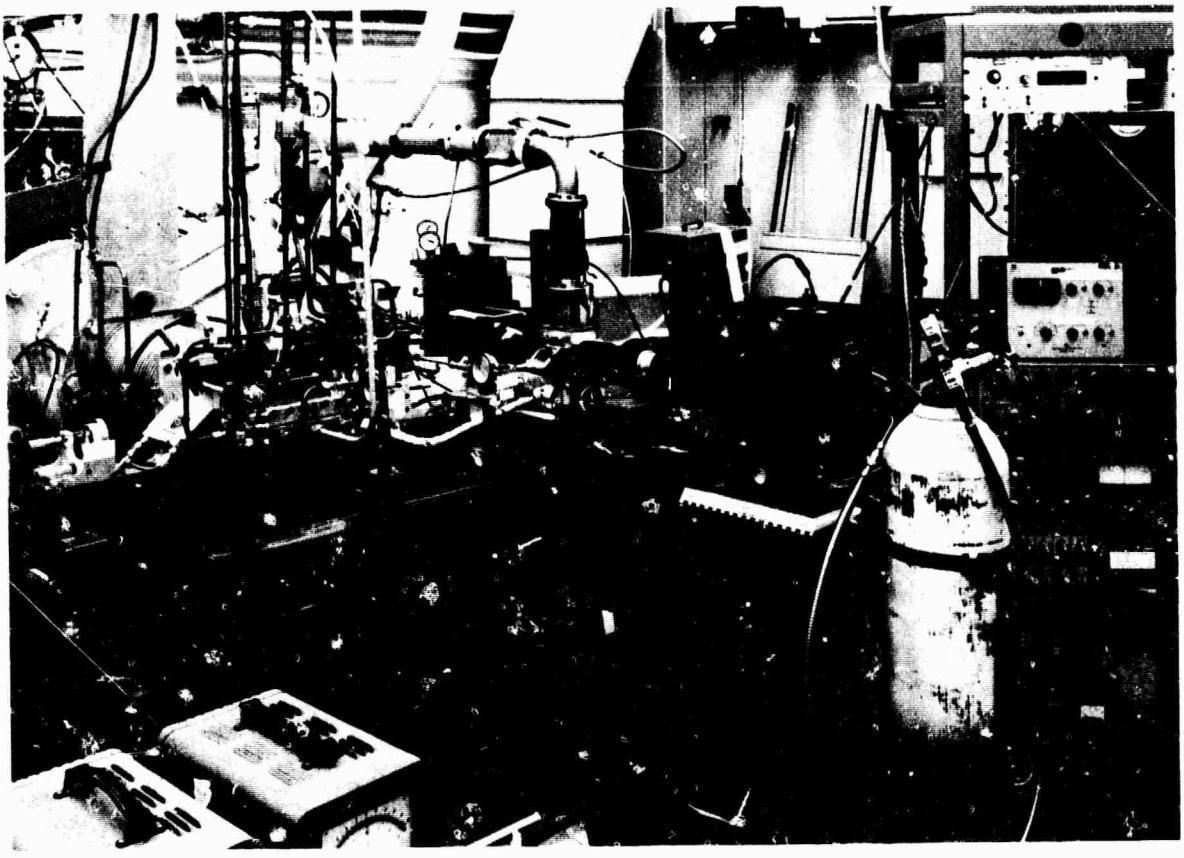

Figure 5. Apparatus for the $DF/CO_2$ fluorescence experiments.

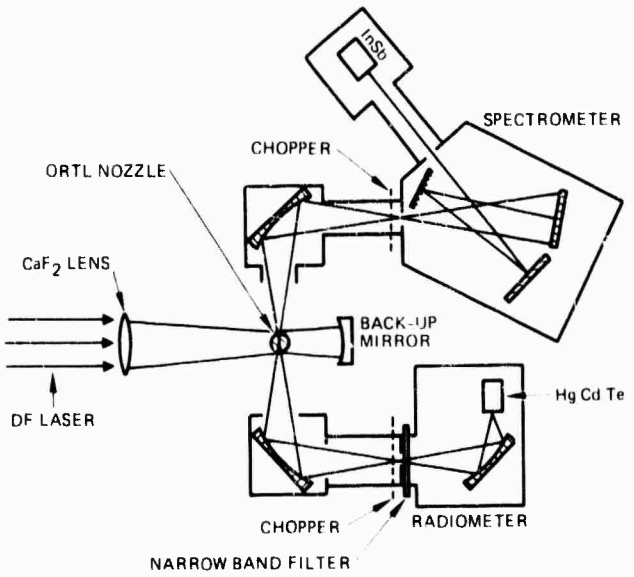


Figure 6. Schematic of the DF/$CO_2$ fluorescence experiments.

laser. The 200 watt DF laser was focused to a 0.7 cm x 0.4 cm cross-section at the interaction zone. A back-up mirror returned the non-absorbed DF radiation to the cell, giving rise to a double pass arrangement. The irradiation flux with optical losses taken into account was 1 kW/$cm^2$. The flow was confined to the duct cross section by a surrounding curtain of helium that matched the pressure and velocity of the DF/$CO_2$/He flow. Emission from both DF and $CO_2$ was detected 90° to the pumping direction by a scanning spectrometer (McPhearson 218) and by a radiometer. Each detection system consisted of a toroidal imaging mirror, a chopper, and a PAR lock-in amplifier utilizing an InSb detector for the spectrometer and HgCdTe detector for the radiometer. In the radiometer two narrow band interference filters (OCLI) centered at the $CO_2$ $(00^0 1)\rightarrow(10^0 0)$ transition at 10.4 μm and the $(00^0 1)\rightarrow$ (000) transition at 4.3 μm were placed alternately in the optical path in order to permit rapid discrimination between fluorescing transitions. The spectrometer was used to determine the DF concentration. It was scanned from 3.2 to 4.2 μm.

The required small flow rates of DF and $CO_2$ were regulated by a calibrated mass flow controller (Matheson model 8249). The helium curtain

and duct flows were controlled by calibrated sonic orifice meters. Typical composition ranged from 0.5 to 2 percent $CO_2$, and 3 to 9 percent DF with He comprising the balance. Such low percentages of $CO_2$ were chosen to maximize the ratio of excited $CO_2$ to total flowing $CO_2$. The cell pressure was selected close to 76 Torr and the velocity was near to $10^4$ cm/sec. The latter was chosen to limit the temperature rise in the gas during irradiation, while the former was detected by mass flow limitations of the vacuum pumps. Some experiments were also performed at 228 Torr, with the velocity consequently lowered to $3.3 \times 10^3$ cm/sec.

## 3.2 DATA REDUCTION METHODS

The DF vibrational population distribution and the gas temperature at the excitation region are determined from analysis of the vibration rotation spectrum obtained by the spectrometer. The line emission intensity, I, originating from the upper level with quantum numbers v'j' integrated along the optical path, $\ell$, is given by

$$I_{v'j'} = \frac{16\pi^3 \nu_o^4 c\ 10^{-7}}{3} \cdot S_{j'} \cdot \left|\mu\right|^2 \frac{\int N_{v'j'} d\mathrm{l}}{2j' + 1} \quad W/cm^2\text{-st} \qquad (1)$$

where $\nu_o$ is the wavenumber ($cm^{-1}$), c is the speed of light, $S_{j'}$ is the rotational line strength factor, $\mu$ is the dipole transition moment, and $N_{v'j'}$ is the number density of the v'j' state. The corresponding signal from the spectrometer is

$$S = I_{v'j'} \cdot \Omega \cdot A \cdot T_\lambda \cdot \alpha_\lambda \qquad \text{Volts} \qquad (2)$$

where S is the signal in volts, $\Omega$ the solid angle subtended by the collection system, A the spectrometer slit area, $T_\lambda$ the transmission factor of all the optical components, and $\alpha_\lambda$ the detector responsivity at wavelength $\lambda$. When the same spectrometer system is calibrated against a blackbody the signal $S_{BB}$ is,

$$S_{BB} = N_{BB} \cdot \Delta\lambda \cdot \Omega \cdot A \cdot I_\lambda \cdot \alpha_\lambda \qquad \text{Volts} \qquad (3)$$

where $N_{BB}$ is the spectral radiance of the blackbody and $\Delta\lambda$ is the resolution of the spectrometer in the units of cm. Substituting the Boltzmann factor for $N_{v'j'}$ in equation (1), and combining equations (1) through (3), we obtain

$$\frac{\int N_{v'j'}dl}{2j'+1} = \frac{e^{-Bj'(j'+1)\frac{hc}{kT}}}{kT/hcB}\int N_{v'}dl = \frac{N_{BB}\cdot\Delta\lambda\cdot S}{[16\pi^3 \times 10^{-7}\nu_o^4 c\, S_{j'}|\mu|^2/3]\cdot S_{BB}} \tag{4}$$

Analysis of equation (4) shows that a plot of $\ln[\int N_{v/j/}dl/(2j'+1)]$ vs $j'(j'+1)$ should be linear provided that self absorption and rotational nonequilibrium effects are negligible. The negative slope of this line equals $hcB/kT$ and the ordinate intercept equals $\ln(hcB/kT)\int N_{v'}dl$. We can therefore determine the temperature from the slope and the DF(v) concentration from the intercept if we assume the path length to equal the diameter of the nozzle.

Analysis of the radiometer signal to obtain $CO_2$ excited state densities differs from that given for the spectrometer insomuch as the interference filter integrates over all emission lines. For the radiometer case we rearrange equation (1) as

$$I_{v'j'} = \left(\frac{16\pi^3\nu_o^4 c\, 10^{-7}\,|\mu|^2 N_{v'}l}{3}\right)\cdot\left[\frac{\left(\frac{\nu'}{\nu_o}\right)^4\cdot S_{j'}\cdot e^{-B'j'(j'+1)\frac{hc}{kT}}}{Q_R}\right] \tag{5}$$

where $N_{v'}$ is the number density of the v' excited state, $Q_R$ is the rotational partion function, and $\nu'$ and B' the wavenumber and rotational constant of the jth state. The signal detected by the radiometer is given by

$$I_{sig} = \left[\sum_{j'} I_{v'j'} f(\lambda)\right]\cdot\Omega\cdot A\,\tau_\lambda\,\alpha_\lambda \tag{6}$$

where the brackets denote the sum over all fluorescing j' states reduced by the appropriate filter transmission factor, $f(\lambda)$. We combine equations (5) and (6), collecting all terms independent of wavelengths.

$$I_{sig} = I_{band} \cdot F(\lambda) \cdot \Omega \cdot A \cdot T_\lambda \alpha_\lambda \tag{7}$$

where $I_{band}$ is the total radiance of the vibrational band. $T_\lambda$ and $\alpha_\lambda$ are assumed to be slowly varying functions of wavelength, and $F(\lambda)$ is given by the fraction of the total band emission transmitted through the filter,

$$F(\lambda) = \frac{1}{Q_R} \sum_{j'} f(\lambda) \left(\frac{\nu_{j'}}{\nu_o}\right)^4 S_{j'} e^{-B'j'(j'+1)hc/kT} \tag{8a}$$

and

$$I_{band} = \frac{16 \pi^3 \nu_o^4 c\, 10^{-7} |\mu|^2 N_{v'} l}{3} \tag{8b}$$

Similarly, the radiometer calibrated against the blackbody yields a signal:

$$I_{BB} = \left| \int_0^\infty N_\lambda f(\lambda)\, d\lambda \right| \Omega A T_\lambda \alpha_\lambda \tag{9}$$

Taking the ratio of eqns. (7) and (9), the factors associated with the radiometer system, $\Omega A T_\lambda \alpha_\lambda$, all cancel. Thus, we have

$$\frac{I_{sig}}{I_{BB}} = \frac{I_{band} \cdot F(\lambda)}{\int_0^\infty N_\lambda f(\lambda)\, d\lambda} \tag{10}$$

We solve for $I_{band}$, and knowing the transition moment of the fluoresceing state, obtain the absolute number density.

Two situations may limit the usefulness of Eq. (10) to derive absolute number densities from data obtained with the radiometer. First, if strong self-absorption is present, an additional term due to self trapping* must be added to Eq. (8). Such is the case if the 4.3 μm $(00^0 1) \rightarrow (000)$ signal were used to infer the $CO_2$ $(00^0 1)$ population. This would greatly complicate the analysis, and render the determination of number densities very questionable. Therefore, we have derived the densities primarily from 10.6 μm data. Secondly, the radiometer counts photons emanating from all transitions that are within the bandpass of the interference filter. Overtones and combination bands at 4.3 μm and 10.6 μm will be transmitted. Hence a determination of absolute numbers densities requires additional information about the relative intensities of these disturbing bands. In spite of these signal analysis problems, we can derive from the measurements meaningful data on $CO_2$ $(00^0 1)$ population densities to satisfy the objectives of this experiment as will be discussed in more detail below.

## 3.3 RESULTS

Fluorescence experiments were performed at DF mole fractions of 3 percent and 6 percent with constant total pressure**. In each case, the $CO_2$ mole fraction was varied. The irradiation flux was 700 $W/cm^2$. Figure 7 shows a plot of the ratio of excited $CO_2$ to total $CO_2$ as a function of $CO_2$ mole fraction at 76 Torr, and Figure 8, shows similar data at 228 Torr. The figures indicate that the region of low $CO_2$ mole fraction is most favorable for 4.3 μm oscillation. Subsequent experiments focused therefore on $CO_2$ mole fractions ranging from 0.5 percent to 2 percent, and DF mole fractions from 1 percent to 9 percent. The pressure and velocity for these experiments was fixed at 76 Torr and $10^4$ cm/sec, respectively.

---

*T. Holstein, Phys. Rev 72, 1212 (1947); 83, 1159 (1951).

**Fourth Monthly Progress Report, Ballistic Missile Defense Advanced Technology Center Contract DASG60-77-C-0056, July, 1977.

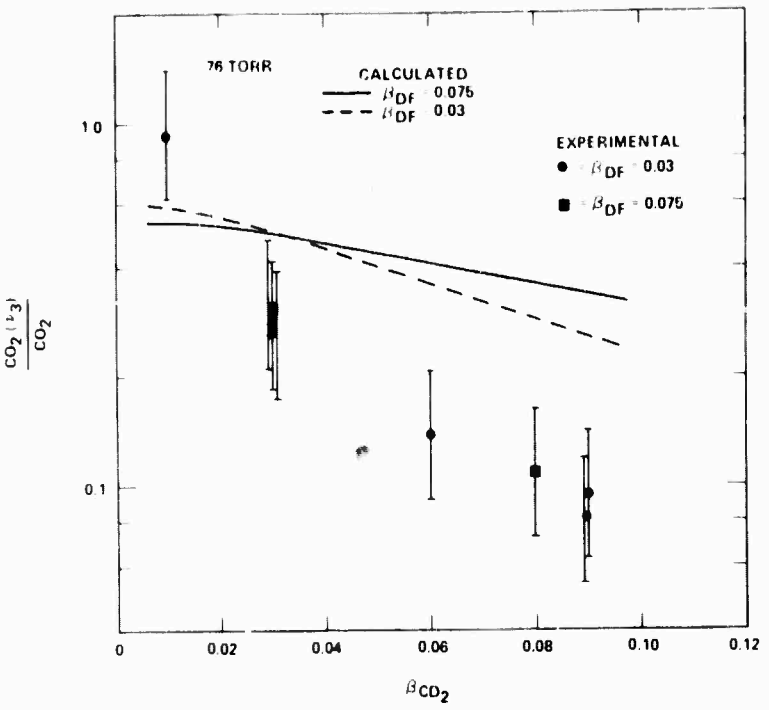


Figure 7. Fluorescence results at 76 Torr (helium diluent).

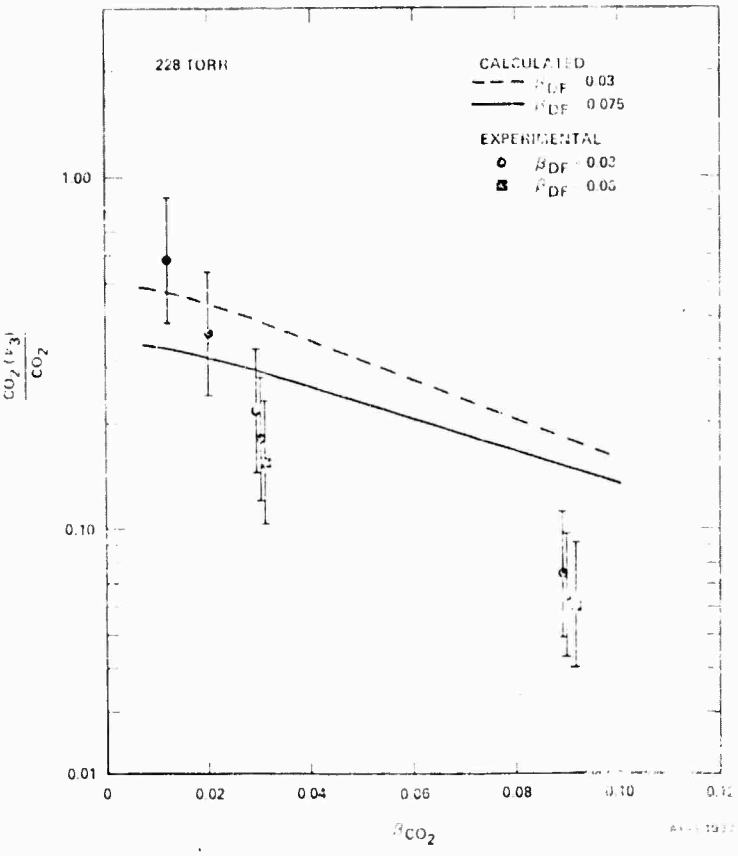


Figure 8. Fluorescence results at 228 Torr (helium diluent).

Signals from both 10.6 μm and 4.3 μm were monitored sequentially by the radiometer. The $CO_2$ ($00^o1$) number density can then be estimated as follows. Recalling Eq. (8b),

$$I_{band} = \frac{16\pi^3 \nu_o^4 c1 \times 10^{-7}}{3} \sum_n \left|\mu_{nm}\right|^2 N_n \tag{11}$$

where $I_{band}$ is written for a multiply fluorescing vibrational manifold. The summation of transition moments can be rewritten as

$$\sum_n \left|\mu_{nm}\right|^2 N_n = \left|\mu_{10}\right|^2 \sum_n \gamma_{nm} N_n \tag{12}$$

where $\gamma_{nm} = \left|\mu_{nm}\right|^2 / \left|\mu_{10}\right|^2$. (For a harmonic oscillator $\gamma_{nm}=n$.) Combining equations (12) and (11) and substituting into Eq. (10), the observed radiometric signal is

$$I_{sig} = K\left|\mu_{10}\right|^2 \sum_{n=1} \gamma_{nm} N_n \tag{13}$$

where K represents all spectroscopic constants, filter factors and black body calibration parameters. Thus the radiometer at 10.6 μm signal may be written as

$$I_{sig}\,(10.6\ \mu m) = K(10.6\ \mu m)\left|\mu_{10.6}\right|^2 \cdot \left[N_1 + \sum_{n=2} \gamma_{nm} N_n\right] \tag{14}$$

where $\mu_{10.6}$ is the moment for the $(00^o1) \rightarrow (100)$ transition. Since every 4.3 μm and 10.6 μm photon emanates from the same common upper level, regardless of the actual upper band distribution, we will assume the same

$\gamma_{nm}$ for both 10.6 μm and 4.3 μm signals. The absorption coefficient for $CO_2$ in air at 4.3 μm is 0.118 $cm^{-1}$ for P(20). For the radiometer air path of 74 cm (it was not purged) the contribution of the $(00^{o}1) \rightarrow (00^{o}0)$ transition is selectively filtered out of the 4.3 μm signal, but the 10.6 μm radiation propagates virtually unattenuated. Thus

$$I_{sig}\ (4.3\ \mu m) = K(4.3\ \mu m) \left|\mu_{4.3}\right|^2 \left[\sum_{n=2} \gamma_{nm} N_n\right] \qquad (15)$$

where $\mu_{4.3}$ is the moment for the $(00^{o}1) \rightarrow (00^{o}0)$ transition.

From Eq. (14) and (15),

$$N_1 = \frac{I_{sig}\ (10.6\ \mu m)}{K(10.6\ \mu m)\left|\mu_{10.6}\right|^2} - \frac{I_{sig}(4.3\ \mu m)}{K(4.3\ \mu m)\left|\mu_{4.3}\right|^2} \qquad (16)$$

The signal strengths obtained in the fluorescence experiment are tabulated in Table I. The data was taken at 76 Torr with $DF/CO_2/He$ mixtures flowing at $10^4$ cm/sec irradiated with a DF flux of 1 $kW/cm^2$. Reduction of the data in Table I, using eq. (16) leads to apparent ratios between the $CO_2$ $(00^{o}1)$ population density and the total $CO_2$ density as follows: For Run Number One, the ratio is 1.5 ±0.75, for Run Two, 1.1 ±0.55, for Run Three, 1.2 ±0.6, and for Run Four, 0.8 ±0.4. The large uncertainty arises from the additive uncertainties associated with gas flow rate control, signal

TABLE I. FLUORESCENCE DATA

| Run | Composition* | | Signal Strength | |
|---|---|---|---|---|
| | $CO_2$% | DF% | $I_{4.3}$ (mV) | $I_{10.6}$ (μV) |
| 1 | 0.6 | 4.0 | 69 | 56 |
| 2 | 1.0 | 7.0 | 70 | 58 |
| 3 | 1.0 | 10.0 | 63 | 52 |
| 4 | 2.0 | 3.0 | 104 | 94 |

*The diluent was helium.

modulation produced by DF laser amplitude modulation, and in temperature measurement. Only values of $[CO_2 (00^0 1)]/[CO_2]$ less than 1 have physical meaning and the fact that the error bars are justified is obvious. In spite of the uncertainties in the experiment, it is apparent that very large population densities are being produced in the $(00^0 1)$ level. The question of whether actual inversion is present depends not on the experimental uncertainties, but rather on the assumptions made in reducing the data. Their validity of course is associated with the precise role of V-V processes in $CO_2$ and the actual vibrational levels which are populated. Fluorescence measurements at other frequencies would assist in determining the population distribution, as would 10.6 μm gain measurements. The critical question of whether or not the $(00^0 1)$ population actually exceeds the inversion conditions is best answered by an appropriate 4.3 μm measurement absorption/gain experiment or by a laser demonstration. In view of the high probability of success indicated by the fluorescence experiments, and the availability of high DF pumping flux the laser demonstration will be attempted first.

# 4.0 LASER DEMONSTRATION EXPERIMENT DESIGN

## 4.1 GENERAL CONSIDERATIONS

In this section we will discuss the design of the 4.3 micrometer laser demonstration experiment. The design parameters are based upon the results of the fluorescence experiments, and existing laboratory equipment will be used as much as possible. The expected small signal gains at both 4.3 and 10.6 micrometers have been estimated. Oscillation at 10.6 μm must be suppressed. (This is easily done with selective reflectivity coatings.) The biggest problem in the experiment design is that of background atmospheric carbon dioxide. Because the desired transition lower laser level is the ground state, unexcited carbon dioxide is a strong absorber. Therefore, this must be excluded from the optical resonator. Small signal gain and absorption calculations will be presented in this section. The apparatus to be used is discussed in Appendix A.

In order to reach the laser oscillation threshold, the small signal gain must be greater than the cavity losses. The small signal gain, $g(\nu_o)$ at line center can be expressed as:

$$g(\nu_o) \quad \frac{8\pi^3}{3h\epsilon} \nu_o S_j |\mu|^2 \left( \frac{N_{v'j'}}{2j'+1} - \frac{N_{v''j''}}{2j''+1} \right) \Gamma(\nu_o) \tag{17}$$

The line profile function $\Gamma(\nu_o)$, in the Doppler domain at line center is given by:

$$\Gamma(\nu_o) = \frac{c}{\nu_o} \sqrt{\frac{M}{2\pi RT}} \tag{18}$$

where M is the molecular weight, and R is the gas constant. If pressure broadening is present, the above equation becomes

$$\Gamma(\nu_o) = \frac{c}{\nu_o}\sqrt{\frac{M}{2\pi RT}} \cdot \left\{ e^{Z^2} \cdot [1 - \mathrm{erf}(Z)] \right\} \tag{19}$$

with Z defined by:

$$Z = (\ln 2)^{1/2} \frac{W_L}{W_D} \tag{20}$$

where $W_L$ and $W_D$ are the Lorentian pressure broadening and Doppler broadening half-width parameters respectively. The number density $N_{vj}$ can be expressed as

$$N_{vj} = \frac{N_v \cdot (2j+1)\, e^{-Bj(j+1)\, hc/kT}}{Q_R} \tag{21}$$

By substituting equations (19) and (21) into equation (17), we obtain for a P-branch line

$$g(\nu_o) = \frac{8\pi^3}{3h} S_j |\mu|^2 \frac{hcB}{kT} \; e^{-Bj''(j''+1)\frac{hc}{kT}}$$

$$\sqrt{\frac{M}{2\pi RT}} \left\{ N_{v'} e^{\frac{2Bj''}{\Gamma}} - N_{v''} \right\} \left\{ e^{Z^2} \cdot [1 - \mathrm{erf}(Z)] \right\} \tag{22}$$

Based upon the fluorescence measurements described previously, the anticipated small signal gain may be estimated for appropriately chosen conditions. Typical laser demonstration experiment conditions are listed in Table II. The DF pump flux will be in excess of 1 kW/cm$^2$. For an anticipated inversion density of $1 \times 10^{16}$ molecules/cm$^3$, the small signal gains at 10.6 μm and 4.3 μm are 1.1 percent per cm and 174 percent per cm respectively.

TABLE II. BASELINE CONDITIONS AND PARAMETERS FOR LASER DEMONSTRATION EXPERIMENTAL ORTL CELL

| | |
|---|---|
| ORTL Mixture: | 93% He<br>6% DF<br>1% $CO_2$ |
| Pressure: | 76 Torr |
| Velocity: | $10^4$ cm/sec |
| Temperature: | 400K |

Linewidths (half width at half maximum):

$\Delta\nu_D$ (10.6 μm) = $1.0 \times 10^{-3}$ $cm^{-1}$

$\Delta\nu_D$ (4.3 μm) = $2.5 \times 10^{-3}$ $cm^{-1}$

$\Delta\nu_L$ = $5.5 \times 10^{-3}$ $cm^{-1}$*

Wavelengths:

$\nu_o$ (18) = 946 $cm^{-1}$ at 10.6 μm

$\nu_o$ (18) = 2335 $cm^{-1}$ at 4.3 μm

Transition moments:

$|\mu|^2$ = $1.5 \times 10^{-39}$ erg $cm^3$ at 10.6 μm**

$|\mu|^2$ = $10^{-37}$ erg $cm^3$ at 4.3 μm***

*R. L. Abrams, Appl. Phys. 25, 609 (1974). We have assumed the same broadening efficiency for DF as for $CO_2$.

**C. Cousin, C. Rosetti, and C. Meyer, Comp. Rend. B 268, 1640 (1969).

***R. A. McClatchey, AFCRL Atmospheric Absorption Line Parameters Compilation, TR-73-0096 (1973).

A closed cavity demonstration experiment is anticipated, where laser oscillation is detected by monitoring the scattering from one of the 4.3 μm resonator mirrors with a radiometer. The total loss will be determined by primarily by residual $CO_2$ absorption and will be about 1 percent. If the above inversion density or slightly more is achieved, laser oscillation at both 10.6 μm and 4.3 μm could be achieved. (The use of coatings with low reflectivity at 10.6 μm is anticipated, to suppress 10.6 μm oscillation.) It is also interesting to calculate the threshold inversion density under these conditions. For a round trip gain length of 6 mm, a 1 percent loss implies an inversion density requirement of $10^{14}$ per $cm^3$ at 4.3 μm and of $1.6 \times 10^{16}$ per $cm^3$ at 10.6 μm to reach threshold. In view of the results discussed in Section 2, such an inversion density is highly probable.

The single most important contribution to loss at 4.3 μm is the presence of unexcited $CO_2$ within the resonator cavity. Sources of unexcited $CO_2$ in the apparatus described in the next section include diffusion out of the irradiated zone, turbulent mixing of the duct and curtain flows, $CO_2$ impurity in the nitrogen gas used to purge the $CO_2$ mirror housings, and leakage of air into the optical path. Extreme care must be taken in order to eliminate each of these sources. In the apparatus described in the appendix, a helium curtain surrounds the active ORTL medium. The curtain extends radially 4.8 mm from the ORTL nozzle walls. The $DF/CO_2/He$ mixture flows so that it is downstream of the excitation zone after 70 μsec. During that time the $CO_2$ can diffuse approximately 0.8 mm in the transverse direction. Therefore laminar diffusion cannot transport any $CO_2$ across the helium curtain. The effect of turbulent diffusion was examined experimentally by sampling the ORTL cell volume outside the helium curtain with a mass spectrometer. The detection limit was 1/1000 of the ORTL flow density. With only $CO_2$ flowing in the nozzle, and the curtain turned on, no $CO_2$ was detected. The typical $CO_2$ impurity level in the nitrogen purge gas is 0.5 ppm or less than $10^{12}$ per $cm^3$ at 76 Torr. The approximate absorption coefficient is $1.74 \times 10^{-16}$ $cm^2$/molecule, leading to an estimated loss of less than 0.01 percent in the proposed experiment. Such a small loss should be easily overcome by the expected gain. A general criterion for successfully overcoming the

absorption problem can be derived. The round trip small signal gain is given by twice the gain length, $L_G$, times the inversion density, $N_{v'}-N_{v''}$, times $1.74 \times 10^{-16}$. This must exceed the actual resonator losses, L, added to the losses due to unexcited $CO_2$. This absorption loss is given by twice the difference between the resonator length, $L_R$, and the gain length, times the unexcited $CO_2$ density, $N_{BKG}$, times $1.74 \times 10^{-16}$. Thus the maximum tolerable unexcited $CO_2$ density is given by

$$2N_{BKG}\,(L_R - L_G)\,1.74 \times 10^{-16} + L = 3.48 \times 10^{-16}\, L_G(N_{v'}-N_{v''})$$

A 4.3 μm resonator will oscillate if

$$N_{BKG} < \frac{L_G(N_{v'}-N_{v''}) - 2.9 \times 10^{17} L}{L_R - L_G}$$

## 4.2 EXPERIMENTAL APPARATUS

The assembly of a new ORTL experimental facility at Hughes has been completed during the reporting period of this contract. While the facility was designed and built around a pre-existing Hughes DF laser, as part of another contract*, this facility will be used for the demonstration experiment on the present program. Specific pieces of hardware for the ORTL cell for this experiment have been funded by the present program. The overall facility is described in Appendix A.

The $CO_2$ ORTL resonator for the 4.3 μm demonstration experiment will consist of a flat 99.8 percent total reflector, and a 1 meter radius dielectric coated concave mirror with 99 percent reflectivity at 4.3 μm, separated by 45 cm. (The concave mirror reflectivity is less than 10 percent at 10.6 μm.) Scatter off the dielectric coating will be imaged onto an InSb detector/radiometer equipped with a 4.3 μm interference filter. Lasing in this geometry is in essence a closed cavity demonstration, with the radiometer serving as the power meter. This concept has been tested with

*Contract DASG60-77-C-0056, sponsored by Ballistic Missile Defense Advanced Technology Center.

a DF laser, and shown to be capable of detecting a 1 μwatt signal. In conjunction with the radiometer, a shutter interposed in the resonator path which will block oscillation, will be used to modulate the radiometer signal. Laser oscillation will be distinguished from fluorescence since for the latter, shuttering the cavity will reduce the radiometer sign by a factor of two. For the former, the factor will be much greater. The entire radiometer path length will be purged with ultrapure $N_2$($CO_2$ < 0.5 ppm).

## 5.0 FUTURE PLANS

### 5.1 IMMEDIATE PLANS

The results of the fluorescence experiments are extremely encouraging. The signal strengths detected indicate that very large fractions of the total $CO_2$ population have been vibrationally excited. In fact under some conditions the fluorescence data indicates that the population inversion required is for 4.3 μm laser oscillation has been achieved. In view of these facts, the most reasonable next step is to attempt to observe 4.3 micrometer laser oscillation. It is anticipated that the required apparatus, as described in Section 4, will be available early in the next stage of this program. Significantly higher DF pump flux than was used in the fluorescence experiments will also be available, if required. Therefore, an attempt at laser oscillation is planned as the next step in the current program.

If this attempt is successful, a series of experiments aimed at characterizing performance as a function of ORTL gas mixture, $CO_2$ concentration, ORTL gas temperature and pressure, and DF pump flux will be undertaken. Additional experiments oriented toward refineing our understanding of the kinetics of the DF:$CO_2$ ORTL system under conditions of high flux irradiation are also being considered. Small signal gain measurements at 10.6 micrometers will be made on another program under similar conditions. This should yield far more reliable data on $CO_2$ ($00^0 1$) population in the absence of lasing than can be obtained from fluorescence experiments. Resonance absorption (or amplification) measurement at 4.3 μm would define the relative ($00^0 0$) and ground state population. In order to do such an experiment, an appropriate source of 4.3 μm radiation must be found. The feasibility of using the fluorescent emission of an electric discharge designed for efficient pumping of a conventional laboratory $CO_2$ laser is being investigated for this purpose.

Information about higher vibrational level population can be obtained by repeating the fluorescence experiments and simultaneously observing the fluorescent emission from higher $\nu_3$ levels, e.g., ($00^0 3$). This can very easily be done and would provide a great deal of information. Of course, such an experiment would not indicate the population densities when laser

oscillation is allowed, but is aimed at understanding the kinetics of this system.

## 5.2 IMPLICATIONS FOR FUTURE WORK

In view of the favorable experimental results obtained so far, and an anticipated successful laser demonstration experiment, it is useful to look ahead toward a possible demonstration of a realistic 4.3 micrometer DF:$CO_2$ ORTL system. A system using a 230 kW DF laser was discussed in the Introduction. However, the basic design concepts and efficiencies can be verified with a much smaller system. Accordingly the ORTL model has been used to generate preliminary design parameters for a laboratory demonstration device which would be large enough to verify efficiency predictions, and beam quality, and which would be amenable to detailed diagnostics. Postulating a 93:6:1 mixture of $H_2$:DF:$CO_2$ operating at one-third atmosphere and 300K with an ORTL cell geometry of 3 cm x 0.3 cm x 0.3 cm (volume = 0.27 $cm^3$), and an inlet Mach number of approximately 0.3, a 50 percent output coupling resonator yields 450 Watts of 4.3 micrometer radiation for an absorbed DF power of 630 Watts. This corresponds to a conversion efficiency of over 70 percent and an output power extraction of 1.66 MWatts/liter. The calculated rise in ORTL gas temperature is only $22^{o}$K. Such a device would serve to verify the model prediction and experimentally demonstrate the usefulness of the 4.3 micrometer DF:$CO_2$ ORTL concept.

## Appendix A. Intacavity ORTL Facility

This facility will permit irradiation of the ORTL cell at flux densities up to 100 KW/cm$^2$. A photograph of the facility is shown in Figure A and a schematic is shown in Figure B. The apparatus is designed to permit either laser or fluorescence experiments to be conducted in the "intracavity" configuration. Pursuant to the above goal the apparatus can accommodate advanced resonator concepts, such as concentric DF laser cavity configurations with spherical or cylindrical mirrors. A summary of the design features of the new facility is listed in Table A.

The apparatus was constructed with three design objectives in mind. The DF resonator necessitated a vibrationally stable platform. The concentric configuration required a stable and resettable resonator distance. Finally, flexibility to change ORTL nozzles, and to run with or without Brewster windows was desired. Vibrational stability was attained by first placing all components on a 4' x 8' vibration isolation optical table. (Newport Research Corp. Model RS-48.) The DF and $CO_2$ mirrors are held in Burleigh mirror mounts, capable of 1 arc second resolution. To permit operation without Brewster windows, the apparatus had to be evacuable. Thus each mirror mount is bolted to a massive (≈50 lb) aluminum base. A Dewar is fitted over each mirror mount, and connected to the DF laser head by bellows. In this manner, vibrations from the laser head or stresses due to evacuation, are transmitted first to the base, and then to the mirror mounts. The design maximum inward deflection for any box cover or wall is 0.003 inch. Each mirror can be adjusted under vacuum through a rotating vacuum feedthrough whose shaft attaches to the mirror mount micrometer via a flexible bellows.

The resonator length is held stable by means of two, 1 inch diameter mirror rods 2 meters in length. The expansion over a 1.5 meter length assuming a 10°F temperature gradient is 13 μm, 20 times less than the limit for stable concentric resonator operation. The Invar rods are attached to the mirror boxes through roller bearings (Thompson) located directly underneath each mirror mount. The mirror housings are able to slide free on the

* This facility was partially funded by Contract DASG60-77-C-0056, sponsored by Ballistic Missile Defense Advanced Technology Center and Hughes Independent Research and Development.

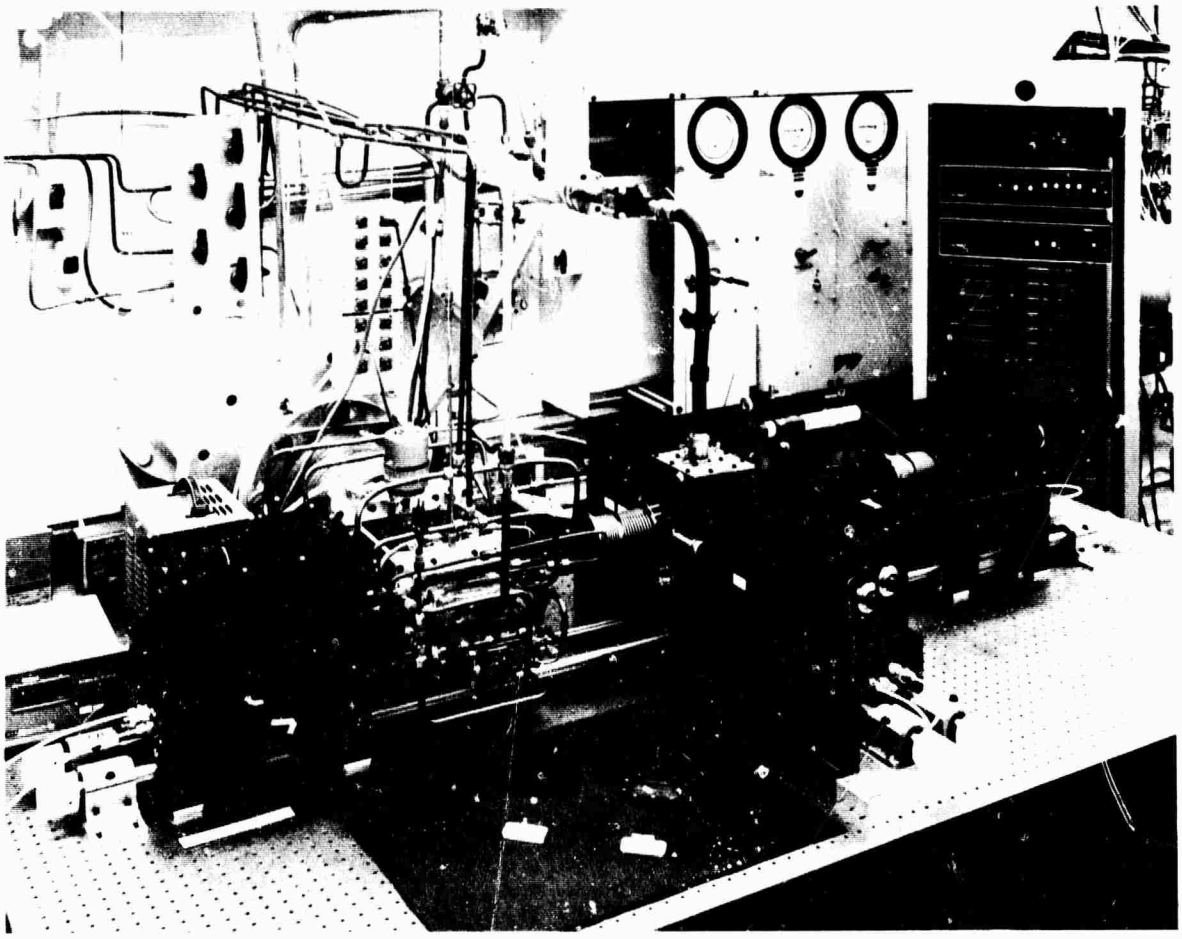

Figure A. Intracavity ORTL Facility.

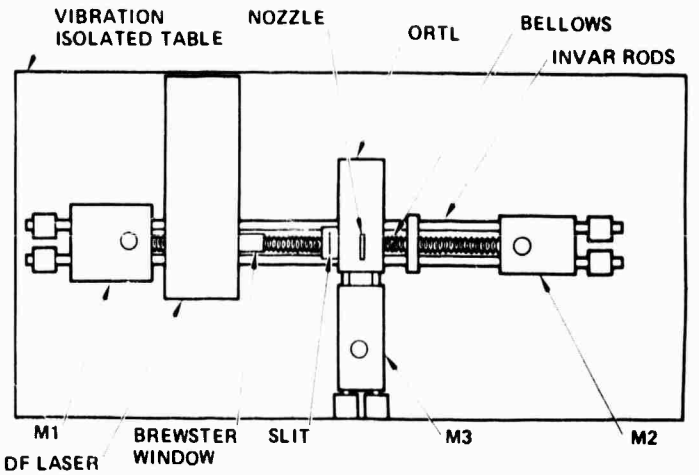


Figure B. Schematic of Intracavity ORTL Facility.

TABLE A. CHARACTERISTICS OF THE NEW INTRACAVITY ORTL FACILITY

| | |
|---|---|
| DF Laser: | |
| DF Laser Resonator length | 150 cm |
| Length stability needed for concentric operation | 300 μm |
| Resonator length change for a $10^{o}$F temperature change | 13 μm |
| ORTL: | |
| Mechanical resonance frequency of the Invar rods | 3 kHz |
| ORTL resonator length | 45 cm |
| Maximum ORTL gain length | 3.0 cm |
| Minimum ORTL gain length | 0.1 cm |
| Intracavity DF Flux:* | |
| 250 W at 7 percent outcoupling | 25 KW/cm$^2$ |
| 1.5 KW at 7 percent outcoupling | 150 KW/cm$^2$ |
| *A focused region of 4 mm x 7 mm is assumed | |

optical table through ball bearing stages located at each corner of the box. In this manner the weight of the boxes is supported by the table, not the mirror, while the separation between the boxes is held constant by the Invar. One of the DF laser mirrors is mounted on a translation stage driven by a PZT translator (Burleigh Inchworm) capable of 0.2 μm resolution and 1 inch extension (see Figure C). Angular orientation can be adjusted manually. In addition, each micrometer is equipped with a PZT pusher which allows continuous adjustment over 150 μradians. Each of these manipulations can be performed under vacuum.

The ORTL cell is modular in construction. Any nozzle or helium curtain smaller than three cm in length can be inserted. The helium curtain is injected radially about the nozzle, so no voids are created when different nozzles are installed. Pressure and temperature of the gas stream is measured through parts located on the ORTL lid. The ORTL flow stream is isolated from the DF laser by a Brewster window.

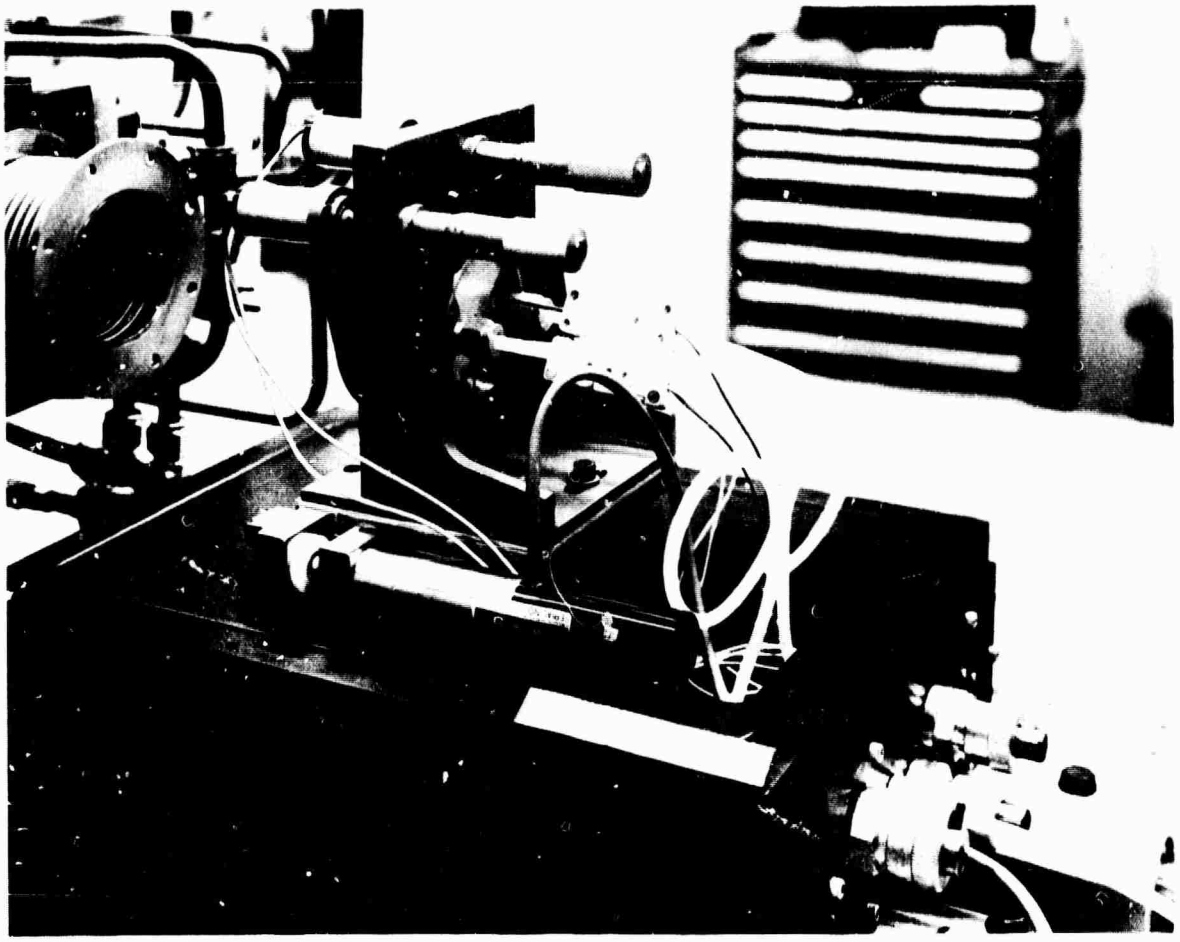

Figure C. DF laser mirror mounting.